

See discussions, stats, and author profiles for this publication at: <https://www.researchgate.net/publication/215969358>

# Unique Temperature Dependence and Blinking Behavior of CdTe/CdSe (Core/Shell) Type-II Quantum Dots

ARTICLE *in* THE JOURNAL OF PHYSICAL CHEMISTRY C · DECEMBER 2010

Impact Factor: 4.77 · DOI: 10.1021/jp109229u

---

CITATIONS

17

READS

55

## 8 AUTHORS, INCLUDING:



Bonghwan Chon

National Institute of Standards and Techno...

26 PUBLICATIONS 415 CITATIONS

[SEE PROFILE](#)



Cherlhyun Jeong

Korea Institute of Science and Technology

25 PUBLICATIONS 191 CITATIONS

[SEE PROFILE](#)



Jong-Bong Lee

Pohang University of Science and Technol...

25 PUBLICATIONS 402 CITATIONS

[SEE PROFILE](#)



Taiha Joo

Pohang University of Science and Technol...

131 PUBLICATIONS 3,965 CITATIONS

[SEE PROFILE](#)

# Unique Temperature Dependence and Blinking Behavior of CdTe/CdSe (Core/Shell) Type-II Quantum Dots

Bonghwan Chon,<sup>†,‡,§</sup> Jiwon Bang,<sup>†,§</sup> Juwon Park,<sup>†</sup> Cherlhyun Jeong,<sup>||</sup> Jong Hwa Choi,<sup>⊥</sup> Jong-Bong Lee,<sup>||</sup> Taiha Joo,<sup>†</sup> and Sungjee Kim<sup>\*,†</sup>

Department of Chemistry and Department of Physics, Pohang University of Science and Technology, San 31, Hyoja-Dong, Nam-Gu, Pohang, 790-784, Korea, and Agency for Defense Development, Neo Technology & Energy R&D Institute, Yuseong P.O. Box 35-4, Daejeon, 305-600, Korea

Received: September 27, 2010; Revised Manuscript Received: November 27, 2010

Temperature dependent photoluminescence (PL) spectroscopy in a range of 5 K to room temperature (RT, 290 K) and single dot blinking behavior were investigated for CdTe/CdSe (core/shell, C/S) quantum dots (QDs). The QDs show type-II characteristics as both of the valence and conduction band levels of the CdTe core are placed higher in energy than those of the CdSe shell. The thickness of the CdSe shell was varied to control the degree of type-II character, and bare CdTe QDs were used as controls. The CdTe/CdSe (C/S) QDs have unique PL properties including (i) high susceptibility to PL thermal quenching with an exciton dissociation energy as small as 18 meV, compared with 46 meV for the CdTe QD, (ii) smaller band gap change showing only half the reduction of the control within the temperature change, and (iii) up to 27% larger PL bandwidth broadening than the control. The unique temperature-dependent properties were enhanced as the type-II character was increased by the thicker CdSe shell. Single dot level PL intermittency characteristics were studied for quasi type-II CdTe/CdSe (C/S) QDs that have alloyed layers at the core–shell interface. The quasi type-II QDs exhibited more frequent PL intensity intermittence blinking on and off at 290 K when compared with the CdTe QDs. However, the blinking kinetics follows similar universal power law on/off probability distributions with the  $\alpha_{\text{on}}$  and  $\alpha_{\text{off}}$  exponents evaluated as 1.57 and 1.38, respectively.

## I. Introduction

In the past decade, zero dimensional semiconductor nano-materials such as quantum dots (QDs) have attracted great interest owing to the unique optical and electrical properties. QDs have proven the potential for various applications including light-emitting-diodes (LEDs),<sup>1,2</sup> lasers,<sup>3</sup> photovoltaic cells,<sup>4</sup> photodetectors,<sup>5,6</sup> bioassays,<sup>7</sup> and bioimaging.<sup>8</sup> Recent development in preparations of colloidal QDs can allow many sophisticated nanostructures like core/shell heterostructures.<sup>9,10</sup> CdSe/ZnS (core/shell, C/S) QDs, for example, can exhibit brighter and more stable emission when compared with bare CdSe QDs. In the case of type-I QDs such as CdSe/ZnS (C/S) QDs, the effective band gaps are mostly governed by the size and composition of the core materials because carriers dwell mostly in the cores. On the other hand, type-II QDs have the conduction and valence band levels of the cores that are offset from those in the shells; hence carriers reside on opposite sides of the core–shell boundary. In CdTe/CdSe (C/S) type-II QDs, holes are mostly confined to the cores and electrons are mostly confined to the shells.<sup>10</sup> Band gaps of the type-II QDs are heavily governed by the band offsets and are typically smaller than either the core or the shell band gap. Due to this unique band alignment, type-II QDs show characteristic optical properties that cannot be paralleled by the type-I counterparts. Type-II QDs

can have spatially separated excitons and can show slow Auger and radiative decay rates,<sup>11</sup> blue shifts of the biexciton energies,<sup>12</sup> very low lasing threshold of single exciton optical gains,<sup>13</sup> and reversible photoluminescence (PL) spectral switching by charging.<sup>14</sup> CdTe/CdSe(C/S) QDs are the most well studied colloidal type-II QDs because they are synthetically well investigated, and because they have many interesting behaviors such as bright luminescence and temperature-dependent emission color changes.<sup>15</sup>

The temperature dependence of QD optical properties can provide insight into the exciton relaxation process and exciton–phonon interactions. Potentials for device applicability of type-II QDs can be evaluated by the temperature dependence studies. For example, type-II QDs can be an optimal active component for photodetectors. QDs have discrete electronic structures that can show reduced dark current and enhanced normal incidence response when compared with quantum well based photodetectors.<sup>16</sup> In addition, type-II QDs can show enhanced photodetector responsivity by the long excited electron lifetime where the photoexcited carriers can efficiently transfer to the electrodes before recombinations can occur.<sup>10</sup> Typically, photodetectors have limitations on the operating temperature because of the change in quantum efficiency resulted from the effective band gap change with temperature<sup>17</sup> and also because of the exponential increase in the thermally excited electron–hole pairs with increasing temperature that results in the boost of dark current.<sup>18</sup> Type-II QDs can be a good candidate material for very sensitive infrared photodetectors with wide operating temperature range. However, the temperature dependence of type-II QDs is still controversial and not fully understood. In the case of a band gap shift of CdTe/CdSe (C/S) type-II QDs, Chin and co-workers have reported that CdTe/CdSe (C/S) type-

\* Corresponding author. Tel: 82-54-279-2108. Fax: 82-54-279-1498. E-mail: sungjee@postech.ac.kr.

<sup>†</sup> Department of Chemistry, Pohang University of Science and Technology.

<sup>‡</sup> Present address: Development 1 Team, Samsung LED 314, Maetan 3-Dong, Yeongtong-Gu, Suwon, 443-743, Korea.

<sup>§</sup> Both authors contributed equally to this work.

<sup>||</sup> Department of Physics, Pohang University of Science and Technology.

<sup>⊥</sup> Neo Technology & Energy R&D Institute.

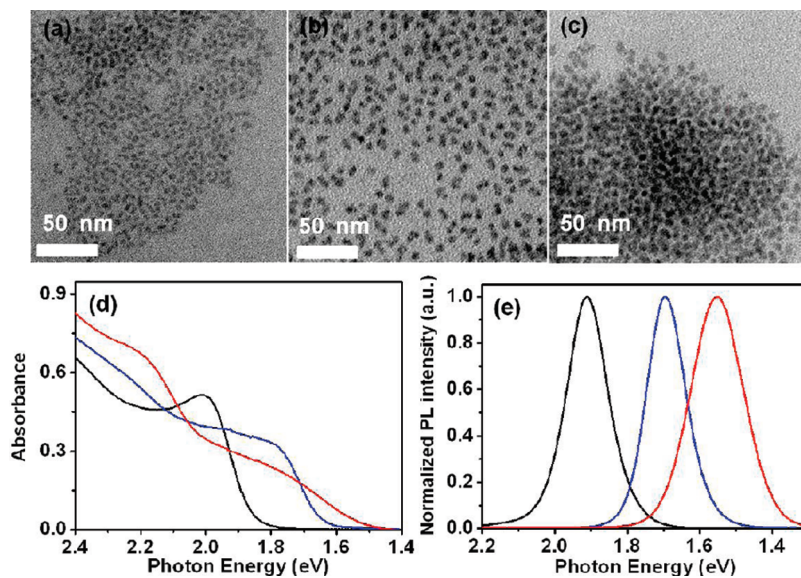


**Figure 1.** TEM images of (a) CdTe core QDs and CdTe/CdSe (core/shell) QDs with shell thicknesses of (b) 1.4 nm (thin shell) and (c) 1.8 nm (thick shell). (d) UV-vis spectra and (e) normalized room temperature PL spectra of CdTe core QDs (black), thin CdTe/CdSe (C/S) type-II QDs (blue), and thick CdTe/CdSe(C/S) type-II QDs (red).

II QDs are less sensitive to the thermal band gap change than CdTe QDs.<sup>15</sup> On the other hand, Wang and co-workers have observed anomalous temperature dependence behavior where CdTe/CdSe (C/S) QDs reversed the direction of the band gap change at 160 K.<sup>19</sup> Inconsistent results have been also reported for the temperature dependent PL bandwidth of CdTe/CdSe (C/S) type-II QDs.<sup>19,20</sup> The blinking behavior of single QD has attracted wide interest for biological imaging<sup>21</sup> and flow cytometry.<sup>22</sup> Recently, Lifshitz and co-workers have reported multiexciton emission and nearly blinking-free behavior for single CdTe/CdSe (C/S) QD by micro-PL studies at 4.2 K.<sup>23,24</sup> This study can be potentially important in biological labeling, gain devices, and photovoltaic cells. However, PL intermittency behavior of single CdTe/CdSe (C/S) QD at RT has not been reported yet.

In the present article, we report temperature dependent PL properties of CdTe/CdSe (C/S) type-II QDs that consist of four properties: PL intensity change, spectral shift of PL, PL broadening, and single dot blinking behavior. The degree of the type-II characteristics has been modulated by the CdSe shell thickness of the sample, and the temperature dependence has been studied as varying the type-II degree. Single QD level PL intermittency was investigated for quasi type-II CdTe/CdSe (C/S) QDs that have alloyed layers at the core–shell interface. We report that type-II CdTe/CdSe (C/S) QDs show unique temperature dependent PL properties of higher susceptibility to PL thermal quenching, smaller band gap change, and larger PL bandwidth broadening than bare CdTe QDs. In addition, quasi type-II QDs exhibited PL intensity flickering on and off intermittently at RT, and the blinking kinetics follows the universal power law on/off probability distribution. We expect that the unique optical properties of the type-II QDs reported herein will advance understanding of QDs and will suggest new applications of QDs.

## II. Experiment

We used methods previously reported<sup>10,14,25</sup> to prepare bare CdTe QDs (average radius 2.3 nm) and two types of CdTe/CdSe (C/S): “thin-shell” (average core radius 2.3 nm, average shell thickness 1.4 nm), and “thick-shell” (average core radius

2.3 nm, average thickness of 1.8 nm). For low temperature experiments, QD films were prepared by drop-casting the growth solution on glass substrates. Slightly opaque QD films that mostly consisted of trioctylphosphine oxide were obtained after drying in ambient condition. PL measurements of the QD films were performed in the temperature (*T*) range 5–290 K by 5 K using a continuous flow liquid He cryostat (Janis, ST-100). The QD films were attached to the sample holder with thermal grease (Apiezon N) to obtain good thermal contact. The light source was a home-built cavity-dumped mode-locked Ti:sapphire laser. The excitation wavelength was 400 nm, which was doubled by the fundamental light (800 nm, 380 kHz, 20 fs) with BBO 100 μm. The 101.6 mm parabolic mirror was used for collecting emissions in the “backscattering” geometry. The PL spectra were collected with a 30 cm monochromator (Acton, SP-300) with a 150 g/mm grating and detected using a charge-coupled device (CCD) (Andor, DV-420). Details of the temperature-dependent PL measurements have been previously reported elsewhere.<sup>26</sup> To observe the blinking dynamics of individual QDs, as-synthesized QDs (~10 pM) were dispersed in 1% (w/v) poly(methyl methacrylate) (MW 15 K) in toluene and spin-cast (2000 rpm, 30 s) on a glass substrate. Room-temperature (290 K) PL properties of individual QDs were investigated using total internal reflection fluorescence microscopy with a 532 nm continuous wave (cw) laser as the excitation source and an electron-multiplying CCD as the detector. For the statistical analysis of QD blinking dynamics, the threshold level for the on/off states was set at 3 times the standard deviation of the averaged background noise.<sup>27</sup>

## III. Results and Discussion

Parts a–c Figure 1 show the transmission electron microscopy (TEM) images of the bare CdTe QDs with the average radius of 2.3 nm, thin-shell CdTe/CdSe (C/S) QDs with the average core radius/shell thickness of 2.3 nm/1.4 nm, and thick-shell CdTe/CdSe (C/S) QDs with the average core radius/shell thickness of 2.3 nm/1.8 nm. Parts d and e of Figure 1 show the absorption and PL emission spectra of the three QD samples as dispersed in hexanes at 290 K. The absorption profiles continue to red shift when comparing shifts from the bare CdTe

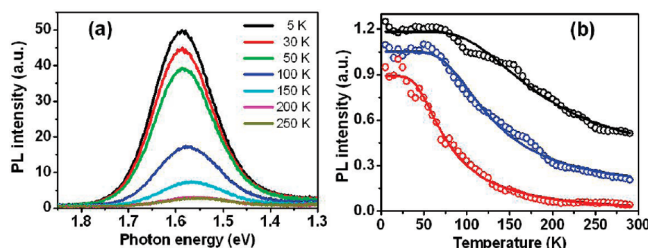


**Figure 2.** (a) PL spectra of thick CdTe/CdSe (C/S) type-II QDs as a function of temperature and (b) Arrhenius plot of PL emission intensities vs temperature in bare CdTe QDs (black), thin CdTe/CdSe (C/S) type-II QDs (blue), and thick CdTe/CdSe (C/S) type-II QDs (red); open circles: the raw data points; solid lines: best least-squares Arrhenius fit (eq 1).

QD sample to thin-shell CdTe/CdSe (C/S) QD and thick-shell CdTe/CdSe(C/S) QD samples, which is characteristic of the enhanced type-II character. The corresponding PL peak wavelengths were 1.55 eV (802 nm), for thick CdTe/CdSe (C/S) QDs, 1.69 eV (734 nm) for thin CdTe/CdSe (C/S) QDs, and 1.91 eV (650 nm) for bare QDs. As the CdSe shell thickness increases, the band levels of the CdTe core are expected to be unchanged whereas the conduction and valence band levels of the CdSe shell are expected to get closer to each other and the carriers feel smaller quantum confinement as the CdSe shell thickens.

**PL Intensity Change.** In temperature dependent PL spectra of thick-shell CdTe/CdSe (C/S) QDs (Figure 2a), the PL peak shapes remain symmetric, as observed in the PLs dispersed in hexanes (Figure 1e); this symmetry suggests that energy transfer between QDs in the film matrix is minimal.<sup>28</sup> As the  $T$  was increased from 5 to 250 K, the PL intensity decreased and the PL emission peak red-shifted. Typically, the radiative channels become more dominant and the effective band gap increases as  $T$  decreases.<sup>15,29–33</sup> Figure 2b shows the plots of PL intensities vs  $T$  for the bare CdTe QD, thin and thick CdTe/CdSe (C/S) QD samples. CdTe/CdSe (C/S) type-II QDs show larger thermal quenching of PL than do bare CdTe QDs. Thick-shell CdTe/CdSe (C/S) QDs are more sensitive to the thermal quenching than the thin-shell CdTe/CdSe (C/S) QDs, presumably because the former have higher type-II character than the latter. The thermal quenching of PL competes with radiative exciton recombination and can be explained in terms of the decomposition of excitons. Using a simple model of a thermally activated transition between two states, the exciton ionization energies ( $I(T)$ ) were evaluated using an Arrhenius fit:

$$I(T) = \frac{I_0}{1 + A \exp\left(-\frac{E_a}{k_B T}\right)} \quad (1)$$

where  $E_a$  is the activation energy that is related to the exciton dissociation,  $A$  is the pre-exponential coefficient, and  $k_B$  is the Boltzmann constant.  $E_a$  was evaluated to be 46 meV for the bare CdTe QDs, 35 meV for the thin-shell CdTe/CdSe (C/S) QDs, and 18 meV for the thick-shell CdTe/CdSe (C/S) QDs. The activation energy for thermal decomposition is inversely proportional to the degree of type-II QD character. As excitons attain larger type-II character, they become more spatially separated and the dissociation activation energy decreases due to the reduced Coulomb interactions between the electron and hole.<sup>34</sup> Morello and co-workers have evaluated the thermal activation energy of 4.9 nm CdTe QDs as 13.6 meV.<sup>31</sup> They have considered the multiple longitudinal optical (LO) phonon

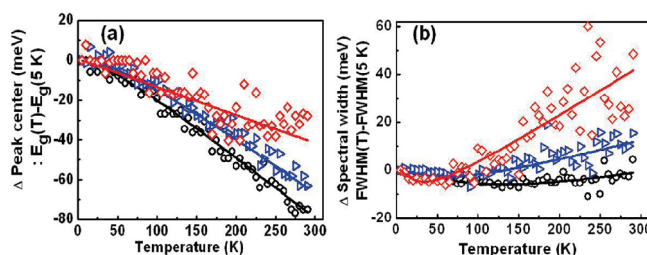


**Figure 3.** (a) Difference of PL peak center (subtracted by the PL energy at 5 K) as a function of temperature and (b) difference of fwhm of the PL (subtracted by the PL fwhm at 5 K) as a function of temperature in CdTe bare QDs (black circles), thin CdTe/CdSe (C/S) type-II QDs (blue square), and thick CdTe/CdSe (C/S) type-II QDs (red diamond).

effect as a separate term. Using the model in ref 16, 4.6 nm CdTe QDs had  $E_a = 8.93$  meV. We speculate that different surface environments in CdTe QDs may have resulted in the discrepancy in the profiles of the tapping sites and the difference in thermal activation energy. Wang and co-workers have evaluated the thermal activation energy using a simple model like ours, and 17.5 meV was obtained for the CdTe/CdSe (3.45 nm average core radius/0.9 nm average shell thickness) sample<sup>19</sup> and 19.2 meV was obtained for the CdTe/CdSe (2.7 nm average core radius/1.0 nm average shell thickness) sample.<sup>20</sup> These values are comparable to that of our thick-shell CdTe/CdSe (average core radius 2.3 nm, average shell thickness 1.8 nm) QDs.

**Spectral Shift of PL.** We also followed the changes of PL energies at the peak center while varying  $T$  from 5 to 290 K. The PL energy at 5 K was subtracted from measured PL energies to reveal the change in band gap with  $T$  (Figure 3a). CdTe/CdSe (C/S) type-II QDs show a smaller band gap change over  $T$  change than did the bare CdTe QDs. Thick-shell CdTe/CdSe (C/S) QDs are less sensitive to the thermal band gap change than the thin-shell CdTe/CdSe (C/S) QDs, presumably due to the greater type-II character. A previous measurement of the thermal sensitivities of the band gap using a bare CdTe QD sample and different shell thickness CdTe/CdSe (C/S) QD samples gave results similar to ours;<sup>15</sup> the authors argued that less strongly temperature dependent CdSe (when compared with CdTe) contributed to the smaller thermal sensitivity of the CdTe/CdSe(C/S) QD band gap as the CdSe shell thickness increased.<sup>15</sup> However, another study observed anomalous temperature dependence behavior of CdTe/CdSe (C/S) QDs in which the direction of the band gap change reversed  $T = 160$  K.<sup>19</sup> Theoretically, band gap changes of QDs should be similar to those of bulk counterparts.<sup>31–33</sup> Anomalous temperature dependences of the PL peak position have been frequently observed in bulk semiconductors, so explaining the unique temperature dependence shown in semiconductor nanostructures is not simple.<sup>35,36</sup> The temperature dependence of the semiconductor band gap is caused by a change in the relative positions of the conduction and valence bands that results from dilatation of the lattice, and from interactions of electrons with the lattice.<sup>29</sup> Type-II QD heterostructures are affected by high internal pressure due to the lattice mismatch between cores and shells, which can make a change of lattice dilatation on the temperature shift. In addition, the carrier radial density distribution of type-II QDs can be changed by the temperature change, which consequently influences the band gap. The two factors can counteract each other, and the temperature dependent band gap shift of type-II QDs is not simple to expect. CdTe/CdSe (C/S) type-II QDs show a smaller change in band gap with  $T$  than do bulk counterparts (Figure 3a). We speculate this partially

**TABLE 1: Best Fit Values Used in the Plot of the Photoluminescence Energy as the Function of Temperature (Figure 3a) Using Eq 2**

Sample	$E_{g,0K}$ (eV)	$\alpha$ (meV/K)	$\beta$ (K)
CdTe	2.02	0.32	66
CdTe/CdSe (thin shell)	1.73	0.29	89
CdTe/CdSe (thick shell)	1.59	0.17	

originated from the temperature-induced atomic interdiffusion across the core–shell boundaries. For CdTe/CdSe (C/S) QDs, the band gaps are strongly influenced by the band offset between the valence level of CdTe and the conduction level of CdSe. Atomic interdiffusion in QDs can be activated at the elevated  $T$ . The temperature dependence of the atomic diffusion coefficient ( $D$ ) can be expressed by an Arrhenius law,  $D(T) = D_\infty \exp(-E_a/k_B T)$ , where  $E_a$  is the activation energy required for a single diffusion process within the crystal lattice.<sup>37</sup> CdTe/CdSe (C/S) heterostructures might partially form CdTeSe-alloyed structures at the core–shell boundaries when  $T$  is high. The alloyed structures may lead to exciton delocalizations and consequent band gap blue shifts.<sup>38</sup> The effective band gap change in excitons with a greater type-II character (and which are thus more spatially separated) should be more sensitive to the effects of CdTeSe alloying process. As the CdSe shell thickness increases in CdTe/CdSe (C/S) QDs, the increased type-II character might have promoted more blue shifts by the alloying process and thus may have reduced sensitivity to the band gap change over  $T$ . In contrast, dilatations of the lattice and reductions in interactions between electrons and the lattice result in band gap red shift as  $T$  increases. The effects of these two factors may offset each other at high  $T$ , and make our type-II QDs less sensitive to changes in  $T$ . In CdTe/CdSe (C/S) type-II QDs, CdTe cores are under compressive stress whereas CdSe shells are under tensile stress because the CdTe has larger lattice cell parameters than does CdSe.<sup>39</sup> The lattice mismatch between the CdTe core and CdSe shell is 6.17%, and the consequent pressure applied to the heterostructure may exceed  $10^9$  Pa.<sup>40</sup> This high internal pressure might have affected the temperature dependence of the band gap in our CdTe/CdSe (C/S) QDs. However, reduction of temperature-dependent lattice dilatations due to the high pressure does not simply explain the smaller temperature sensitivity of type-II CdTe/CdSe (C/S) QDs, because CdSe/ZnS (C/S) QDs that should be subjected to similar pressure as our type-II QDs have been reported to show temperature dependent band gap changes that are similar to those in the bulk counterpart.<sup>33</sup> The temperature dependence of the experimental PL peak center in a bulk semiconductor can be modeled by the Varshni relation:<sup>29</sup>

$$E_g(T) = E_{g,0K} - \frac{T^2}{(T + \beta)} \quad (2)$$

where  $E_g(T)$  is the PL peak center as the function of absolute temperature  $T$ ,  $E_{g,0K}$  is the band gap (PL peak center) at 0 K,  $\alpha$  is a temperature coefficient, and  $\beta$  is approximately the Debye temperature of the semiconductor. Equation 2 is based on the temperature-dependent dilatation of lattice and the interactions between lattice phonon and exciton.<sup>29,30</sup> Parameters were extracted for the CdTe QDs, and for thin-shell and thick-shell CdTe/CdSe (C/S) QD samples (Table 1). In plots of peak shift vs  $T$  (Figure 3a), the absolute magnitude of the slope decreases as QDs attain more type-II characters. The fitted  $\alpha$  value for CdTe QDs was close to the bulk value (0.3 meV/K),<sup>41</sup> but the

fitted  $\alpha$  value decreased for type-II CdTe/CdSe (C/S) QDs. The  $\alpha$  value of bulk CdSe is similar to that of CdTe.<sup>41</sup> The decrease in  $\alpha$  values in type-II QDs correlates well with the temperature insensitivity of the band gap in our CdTe/CdSe (C/S) QDs. The  $\beta$  values evaluated were 66 K for CdTe QD and 89 K for thin-shell CdTe/CdSe (C/S) QD samples. These values are comparable to the known values of CdTe QDs (102 K)<sup>15</sup> and various CdSe nanostructures (78–162 K).<sup>32</sup> The  $\beta$  value for thick-shell CdTe/CdSe (C/S) QDs could not be estimated due to data fluctuation. The relatively temperature-insensitive PL properties of CdTe/CdSe (C/S) type-II QDs can open potential applications for many optoelectronic devices that require high thermal stability in the spectral emission.

**PL Broadening.** Full width at half-maximum (fwhm) of the PL spectrum was plotted vs  $T$  for CdTe QD, and for thin-shell and thick-shell CdTe/CdSe (C/S) QD samples (Figure 3b). The fwhm of CdTe QDs was quite insensitive to  $T$ , but that of CdTe/CdSe (C/S) type-II QDs showed nonmonotonic temperature dependence. Below a critical temperature, the fwhm decreased slightly as the temperature increased. As the temperature exceeds the critical temperature, the fwhm increased rapidly with a slope proportional to the type-II character. The critical temperatures were measured as 60 and 35 K, respectively, for the thin and thick CdTe/CdSe(C/S) QDs. The temperature dependence of the PL bandwidth of our CdTe/CdSe (C/S) type-II QDs was quite different from those observed in previous reports. In one previous study, CdTe/CdSe (C/S) QDs (average core radius 3.45 nm, average shell thickness 0.9 nm) QDs, fwhm first increased and later decreased as  $T$  was raised from 15 to 300 K; the change of direction occurred at 200 K.<sup>19</sup> The authors argued that the thermal broadening mostly contributed at low  $T$  and that the effect of carrier accumulation effect began at high  $T$ . Interestingly, the same group later reported similar experiments where the fwhm of CdTe/CdSe (2.7 nm average core radius/1.0 nm average shell thickness) QDs showed the monotonously increased PL fwhm as the elevating  $T$ .<sup>20</sup> The PL bandwidth of a QD sample is determined by the convolution of inhomogeneous broadening due to the size and shape distributions, and by homogeneous broadening that originates from the scattering of excitons by LO phonons and by acoustic phonons. Due to the phonon effect, the PL bandwidth is expected to broaden in bulk semiconductors and also in QDs.<sup>31–33,42</sup> The measured bandwidth of the CdTe QD sample PL spectrum at 5 K was 160 meV and was quite insensitive to changes in  $T$ . This insensitivity suggests that the PL bandwidth is mostly due to inhomogeneous broadening. On the other hand, Morello and co-workers have observed the broadening of PL bandwidth for CdTe QD samples as elevating the  $T$ .<sup>31</sup> It is noted that their CdTe QDs had very narrow size distributions with the PL bandwidth of ~50 meV at 15 K. The minimal inhomogeneous broadening may have revealed the temperature-dependent broadening effect of homogeneous broadening. In contrast, our CdTe sample has a relatively large size distribution, and the inhomogeneous broadening may have overwhelmed any temperature-dependent PL bandwidth changes. As a result, the PL fwhm of the CdTe QD sample appeared to be independent of  $T$ . The FWHMs of the thin and thick CdTe/CdSe(C/S) type-II QD sample PL spectra were fitted to the following equation:<sup>42</sup>

$$\Gamma(T) = \Gamma_{inh} + \sigma T + \Gamma_{LO}(e^{E_{LO}/k_B T} - 1)^{-1} \quad (3)$$

where  $\Gamma_{inh}$  is inhomogeneous broadening,  $\sigma$  is the exciton-acoustic-phonon coupling coefficient,  $\Gamma_{LO}$  is the exciton-LO-

**TABLE 2: Best Fit Values Used in the Fit of the FWHM of the PL as a Function of Temperature (Figure 3b) with Eq 3**

Sample	$\Gamma_{\text{inh}}$ (meV)	$\alpha$ ( $\mu\text{eV/K}$ )	$\Gamma_{\text{LO}}$ (meV)	$E_{\text{LO}}$ (meV)
CdTe/CdSe (thin shell)	124	-60.3	37.6	20.8
CdTe/CdSe (thick shell)	157	-429	43.3	5.92

phonon coupling coefficient,  $E_{\text{LO}}$  is the LO phonon energy, and  $k_B$  is the Boltzmann constant. In eq 3,  $\Gamma_{\text{inh}}$  is temperature independent and is related to the heterogeneity of the nanocrystal size, shape or composition;  $\sigma T$  is a bandwidth that changes linearly with  $T$ ; the third term contains an exponential function that is related to the Boltzmann distribution and is highly dependent on  $T$ . Parameters in eq 3 were estimated for the thin-shell and thick-shell CdTe/CdSe (C/S) QD samples (Table 2). Calculated  $\Gamma_{\text{inh}}$  was 124 meV for the thin-shell CdTe/CdSe (C/S) QDs and 155 meV for the thick-shell CdTe/CdSe (C/S) QDs. Our CdTe/CdSe (C/S) type-II QDs show slight bandwidth reduction before they reach the critical point. This reduction may occur because the thermally induced excitons, which are accumulated in the localized states, radiatively recombine with a similar energy.<sup>19</sup> The thick-shell CdTe/CdSe (C/S) QD sample may have a higher density of states near the band edge than the thin sample. As a result, excitons in thick-shell CdTe/CdSe (C/S) QDs should need less thermal energy to accumulate in the localized states than do thin-shell CdTe/CdSe (C/S) QDs, and thus the thick-shell type-II QD sample has a lower critical temperature than the thin-shell sample. This local state coupled exciton effect predominates at low temperatures and may have masked the acoustic phonon effect. The acoustic phonon coupling constants  $\sigma$  were negative in both thin-shell and thick-shell CdTe/CdSe (C/S) QDs. We think that the negative values hold no practical meaning and consider them to be the consequence of the insignificant effect of acoustic phonon coupling compared with local state exciton coupling. At the points above the critical temperature, a rapid increase in bandwidth was observed for both thin-shell and thick-shell CdTe/CdSe (C/S) QD samples. As  $T$  was raised from 5 and 290 K, the PL bandwidth was broadened by 15 meV in the thin-shell CdTe/CdSe (C/S) QD sample and by 42 meV in the thick-shell CdTe/CdSe (C/S) QD sample. At this temperature region, the bandwidth is considered to be heavily governed by the LO phonon coupling. Extracted LO phonon energies were 20.8 meV for the thin-shell CdTe/CdSe (C/S) QDs and 5.92 meV for the thick-shell CdTe/CdSe (C/S) QDs. Vinogradov and co-workers have reported the LO phonon energies of 25.5 and 20.8 meV for CdTe/CdSe(C/S) QDs that corresponded to the CdSe and CdTe, respectively.<sup>43</sup> LO phonon energies are 26.1 meV in bulk CdSe and 21.1 meV in bulk CdTe.<sup>41</sup> In general, the LO phonon energy should be independent of the nanostructures when the internal strain is ignored. We believe that the smaller LO phonon energies obtained for our CdTe/CdSe(C/S) QDs compared with the previously published values originate from the overcompensation for the enhanced type-II exciton–LO phonon couplings in our fitting. Our estimated coupling constants  $\Gamma_{\text{LO}}$  were 37.6 meV for the thin-shell CdTe/CdSe (C/S) QDs and 43.3 meV for the thick-shell CdTe/CdSe (C/S) QDs. These values are significantly larger than the theoretical bulk values of 18.3 meV for CdSe and 24.5 meV for CdTe.<sup>44</sup> LO phonon coupling energies have been reported as 24.5 meV for CdSe QDs and 14–21 meV for CdTe QDs.<sup>31,33</sup> Spatially separated excitons in CdTe/CdSe (C/S) QDs can be highly polarized, and the localized excitons may increase the Fröhlich coupling between the exciton and optical phonon.<sup>45,46</sup> As a result, PL bandwidth broadening by the nonlinearly temperature-

dependent exciton–LO phonon scattering prevails in CdTe/CdSe (C/S) QDs when  $T$  is high. Compared with the thin-shell CdTe/CdSe (C/S) QD, the thick-shell CdTe/CdSe (C/S) QD sample has greater type-II character and thus has larger LO coupling energy. Due to the unique interactions of type-II excitons with localized states and LO phonons, or both, CdTe/CdSe (C/S) type-II QDs show the peculiar characteristic that the effective band gap energy is insensitive to  $T$  whereas at the same time the PL bandwidth is highly sensitive to  $T$ .

**Single Dot Blinking Behavior.** Fluorescence of single QD intermittently flickers on and off. The fluorescence intermittency in single QD is considered to be caused mainly by repeated ionization or trapping followed by neutralization in the QD.<sup>27,47–57</sup> In the on state, the QD is neutral in charge and the photoexcited excitons can recombine radiatively. The off state is believed to occur when electrons or holes are ejected from the QD and trapped in the surface or in defects in the surrounding matrix. As a result, the QD becomes ionized, and the photoexcited excitons decay by predominantly nonradiative mechanisms. The on/off probability distributions of various QDs follow a universal power-law,  $P(T) = At^{-\alpha}$ , with switching intervals from milliseconds to minutes regardless of the QDs' size,<sup>48</sup> shape,<sup>49</sup> lattice structure,<sup>50</sup> shell composition,<sup>49,51,52</sup> surface passivating ligand,<sup>51</sup> temperature,<sup>53</sup> and the excitation power.<sup>49</sup> Typical  $\alpha$  values fall between 1 and 2 for both on and off times. To explain the universal power-law probability distribution of single QD emission intermittency, several models are proposed. The early ionization based on/off model was suggested by Efros and Rosen.<sup>54</sup> To explain the deviation of the on/off distribution from the expected exponentials, other models have been introduced such as multiple trap,<sup>55</sup> spectral diffusion,<sup>56</sup> spatial diffusion,<sup>57</sup> and fluctuating barrier model.<sup>27</sup> However, the complete mechanism that causes QD blinking is still unknown. In this work, we have aimed to compare the blinking behavior of CdTe/CdSe (C/S) QDs in single dots as compared with the counterpart bare CdTe QDs. Following the single QD level emission properties was very difficult in the type-II CdTe/CdSe (C/S) QDs that we used for the temperature dependence measurement. The signal-to-noise ratio was very low, and sufficient data could not be accumulated because the QDs were very vulnerable to photobleaching. Therefore, we synthesized small CdTe QDs (2.7 nm diameter) by modifying the preparation conditions,<sup>25</sup> then slowly deposited CdSe shells onto the small CdTe QDs. Small CdTe QDs were chosen because the high surface energy can easily promote formation of CdTeSe at the interface between the core and the shell. The resultant CdTe/CdSe (C/S) QDs had brighter PL and were less sensitive to photobleaching than were typical type-II QDs. The assumption of the CdTeSe alloyed layers, which is based on the preparation condition, can explain the increased PL. We call these CdTe/CdSe (C/S) QDs “quasi type-II CdTe/CdSe (C/S) QDs” because we speculate that they will show less type-II character due to the alloyed CdTeSe interface.

Absorption and PL spectra were obtained for the small CdTe QD and the quasi type-II CdTe/CdSe (C/S) QD sample (Figure 4a). In the absorption spectrum, the quasi type-II CdTe/CdSe (C/S) QDs show the red-shifted and the band-edge attenuated profile, which is characteristic of type-II QDs.<sup>10</sup> The emission spectrum also red-shifts as the PL bandwidth broadens significantly. Based on the TEM measurements as shown in Figure 4b, our quasi type-II CdTe/CdSe(C/S) QDs have the average diameter of 5.1 nm with the relative size distribution of 9.89%. The small bare CdTe QDs show the relative size distribution of 17.1%. The quasi type-II CdTe/CdSe (C/S) QDs have a PL bandwidth of 164 meV, which is wider than that of the small

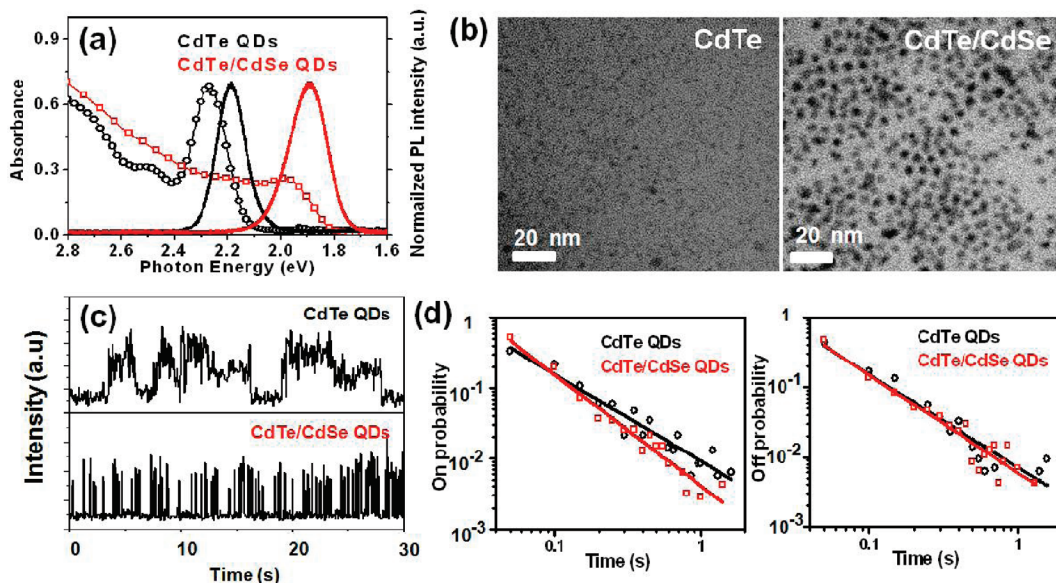


**Figure 4.** (a) UV-vis spectra (line with open symbol) and normalized room temperature PL spectra (line) of bare CdTe QDs (black) and quasi-type-II CdTe/CdSe(C/S) QDs (red). (b) TEM images of bare CdTe QDs and quasi-type-II CdTe/CdSe(C/S) QDs. (c) Typical fluorescence time traces from individual bare CdTe QD and quasi-type-II CdTe/CdSe(C/S) QD. Each time trace is 30 s long with 50 ms bin time. The data were extracted from continuous 5 min measurements. (d) On- and off-time probability distributions of individual bare CdTe QDs (black, circle) and quasi-type-II CdTe/CdSe(C/S) QDs (red, square).

CdTe QDs (124 meV) even though the size distribution of the former is narrower than that of the latter. The PL bandwidth in QDs is predominantly determined by inhomogeneous broadening. In the quasi type-II CdTe/CdSe (C/S) QDs, the inhomogeneity becomes the convolution of the core size and the shell thickness. As a result, the quasi type-II CdTe/CdSe (C/S) QDs can show broader PL bandwidth despite the narrower size distribution than that of small CdTe QDs. This confirms the type-II character of our quasi-type-II CdTe/CdSe (C/S) QDs and excludes the possibility that the entire QD is made of homogeneous CdTeSe alloy.

Typical single QD fluorescence time traces were collected in bins of 50 ms for the CdTe QD and quasi-type-II CdTe/CdSe (C/S) QD samples (Figure 4c). Both samples show bimodal on/off behavior. The PL of our quasi type-II CdTe/CdSe (C/S) QDs exhibits frequent PL intensity intermittence blinking on and off at RT. Lifshitz and co-workers have observed multiexciton emissions and nearly blinking-free behavior of single quasi type-II CdTe/CdSe (C/S) QDs by micro-PL spectroscopy at 4.2 K. The CdTe/CdSe (C/S) QDs showed suppressed nonradiative Auger recombinations at the low temperature.<sup>23,24</sup> However, the single dot blinking behavior for type-II QDs has not been reported yet for RT. Our quasi type-II CdTe/CdSe (C/S) QD samples show frequent PL intermittency at RT. The thermally activated excitons in the quasi type-II CdTe/CdSe (C/S) QDs may escape from the QDs, encounter the trap sites, and return to the neutral state after temporary residence in the traps. As shown in Figure 2b, the type-II excitons have reduced electron–hole wave function overlaps and thus the dissociation energy is smaller than that of CdTe QDs. As a result, the shell-localized electrons in the quasi-type-II CdTe/CdSe (C/S) QDs are more susceptible to the trap sites before they recombine with the holes in the CdTe cores. The CdSe shells can have trap sites on both the inner and outer interfaces, which may provide the electrons with frequent accesses to shallow traps. This can result in the quasi type-II CdTe/CdSe (C/S) QDs capturing the photoexcited excitons more frequently, thus showing shorter periods of continuous emission

than the CdTe QDs. The probability distributions for the two samples are plotted in Figure 4d. Both samples show on and off time distributions that agree well with the power law. For the CdTe QD sample, the on time exponent ( $\alpha_{on}$ ) was  $1.41 \pm 0.01$  and the off time exponent ( $\alpha_{off}$ ) was  $1.38 \pm 0.01$ . In the quasi type-II CdTe/CdSe (C/S) QD sample,  $\alpha_{on}$  was  $1.57 \pm 0.01$  and  $\alpha_{off}$  was  $1.38 \pm 0.01$ . The CdTe QD and quasi type-II CdTe/CdSe (C/S) QD samples showed the same value of off time exponent. The transition from the dark to the bright state can be described as a tunneling process that is not photoassisted. This process causes the QD blinking off time distributions to conform closely to the power law regardless of the temperature, excitation intensity, surface morphology or the dot size.<sup>53</sup> In both the CdTe and the quasi-type-II CdTe/CdSe (C/S) QDs, the trapped or ejected carriers seem to hop back to the bright state by similar tunneling processes, and to have very similar off time statistics. The value of  $\alpha_{on}$  was slightly greater for the quasi-type-II QD sample than for the CdTe QD sample; however, the values did not significantly deviate from each other. The measured exponent values fall within the same range reported in previous single QD blinking measurements.<sup>48–57</sup> The simple power law that governs most QDs blinking behavior can be extended to our quasi type-II CdTe/CdSe (C/S) QDs. The blinking kinetics of the quasi type-II CdTe/CdSe (C/S) QD follows the universal power law despite their unique PL properties such as slow Auger and radiative decay rates<sup>9</sup> and the distinctive temperature dependence that we report in this paper.

## Conclusions

In summary, we have performed the temperature dependent PL spectroscopy and single dot blinking behavior investigations of CdTe/CdSe(C/S) QDs. The thickness of the CdSe shell was varied to control the degree of type-II character; bare CdTe QDs were used as controls. The CdTe/CdSe (C/S) QDs have unique PL properties including higher susceptibility to the PL thermal quenching, smaller band gap change, and PL bandwidth broadening over temperature than do bare CdTe QDs. The

unique temperature dependent properties became more pronounced as the type-II character was increased by thickening the CdSe shell. Single-dot level PL intermittency behavior were studied for quasi type-II CdTe/CdSe (C/S) QDs; in these QDs PL intensity flickered on and off intermittently at RT. The blinking kinetics follows the universal power law on/off probability distribution with  $\alpha_{\text{on}} = 1.57$  and  $\alpha_{\text{off}} = 1.38$ .

**Acknowledgment.** This work was supported by the Korea Science and Engineering Foundation (KOSEF) grant funded by the Korea government (MOST) (20100018467) (20100020649), Priority Research Centers Program through the National Research Foundation of Korea (NRF) (2009-0094037), Defense Acquisition Program Administration and Agency for Defense Development under the contract ADD-08-11-03, and the Korea Research Foundation Grant funded by the Korean Government (MOEHRD, Basic Research Promotion Fund) (KRF-2008-313-2-C00364).

## References and Notes

- (1) Coe, S.; Woo, W. K.; Bawendi, M.; Bulovic, V. *Nature (London)* **2002**, *420*, 800.
- (2) Tessler, N.; Medvedev, V.; Kazes, M.; Kan, S. H.; Banin, U. *Science* **2002**, *295*, 1506.
- (3) Eisler, H. J.; Sundar, V. C.; Bawendi, M. G.; Walsh, M.; Smith, H. I.; Klimov, V. *Appl. Phys. Lett.* **2002**, *80*, 4614.
- (4) Greenham, N. C.; Peng, X. G.; Alivisatos, A. P. *Phys. Rev. B* **1996**, *54*, 17628.
- (5) Konstantatos, G.; Howard, I.; Fischer, A.; Hoogland, S.; Clifford, J.; Klem, E.; Levina, L.; Sargent, E. H. *Nature (London)* **2006**, *442*, 180.
- (6) Clifford, J. P.; Konstantatos, G.; Johnston, K. W.; Hoogland, S.; Levina, L.; Sargent, E. H. *Nat. Nanotechnol.* **2009**, *4*, 40.
- (7) Bruchez, M.; Moronne, M.; Gin, P.; Weiss, S.; Alivisatos, A. P. *Science* **1998**, *281*, 2013.
- (8) Bhang, S. H.; Won, N.; Lee, T.-J.; Jin, H.; Nam, J.; Park, J.; Chung, H.; Park, H.-S.; Sung, Y.-E.; Hahn, S. K.; Kim, B.-S.; Kim, S. *ACS Nano* **2009**, *3*, 1389.
- (9) Peng, X.; Schlamp, M. C.; Kadavanich, A. V.; Alivisatos, A. P. *J. Am. Chem. Soc.* **1997**, *119*, 7019.
- (10) Kim, S.; Fisher, B.; Eisler, H. J.; Bawendi, M. *J. Am. Chem. Soc.* **2003**, *125*, 11466.
- (11) Oron, D.; Kazes, M.; Banin, U. *Phys. Rev. B* **2007**, *75*, 035330.
- (12) Ivanov, S. A.; Nanda, J.; Piryatinski, A.; Achermann, M.; Balet, L. P.; Bezel, I. V.; Anikeeva, P. O.; Tretiak, S.; Klimov, V. I. *J. Phys. Chem. B* **2004**, *108*, 10625.
- (13) Klimov, V. I.; Ivanov, S. A.; Nanda, J.; Achermann, M.; Bezel, I.; Mc Guire, J. A.; Piryatinski, A. *Nature (London)* **2007**, *447*, 441.
- (14) Bang, J.; Chon, B.; Won, N.; Nam, J.; Joo, T.; Kim, S. *J. Phys. Chem. C* **2009**, *113*, 6320.
- (15) Chin, P. T. K.; de Mello Donega', C.; van Bave, S. S.; Meskers, S. C. J.; Sommerdijk, N. A. J. M.; Janssen, R. A. J. *J. Am. Chem. Soc.* **2007**, *129*, 14880.
- (16) Liu, H. C. *Opto-Electron. Rev.* **2003**, *11*, 1.
- (17) Edmond, J.; Kong, H.; Suvorov, A.; Waltz, D.; Carter, C., Jr. *Phys. Status Solidi A* **1997**, *162*, 481.
- (18) Józwikowski, K.; Kopytko, M.; Rogalski, A.; Józwikowska, A. *J. Appl. Phys.* **2010**, *108*, 074519.
- (19) Wang, C. H.; Chen, T. T.; Tan, K. W.; Chen, Y. F.; Cheng, C. T.; Chou, P. T. *J. Appl. Phys.* **2006**, *99*, 123521.
- (20) Wang, C. H.; Chen, T. T.; Chen, Y. F.; Ho, M. L.; Lai, C. W.; Chou, P. T. *Nanotechnology* **2008**, *19*, 115702.
- (21) Medintz, I. L.; Uyeda, H. T.; Goldman, E. R.; Mattoussi, H. *Nat. Mater.* **2005**, *4*, 435.
- (22) Chattopadhyay, P. K.; Price, D. A.; Harper, T. F.; Betts, M. R.; Yu, J.; Gostick, E.; Perfetto, S. P.; Goepfert, P.; Koup, R. A.; De Rosa, S. C.; Bruchez, M. P.; Roederer, M. *Nat. Med.* **2006**, *12*, 972.
- (23) Osovsky, R.; Cheskis, D.; Kloper, V.; Sashchiuk, A.; Kroner, M.; Lifshitz, E. *Phys. Rev. Lett.* **2009**, *102*, 197401.
- (24) Kloper, V.; Osovsky, R.; Cheskis, D.; Sashchiuk, A.; Lifshitz, E. *Phys. Status Solidi C* **2009**, *6*, 2719.
- (25) Smith, A. M.; Nie, S. J. *Am. Chem. Soc.* **2008**, *130*, 11278.
- (26) Lim, S. J.; Chon, B.; Joo, T.; Shin, S. K. *J. Phys. Chem. C* **2008**, *112*, 1744.
- (27) Kuno, M.; Fromm, D. P.; Hamann, H. F.; Gallagher, A.; Nesbitt, D. *J. J. Chem. Phys.* **2001**, *115*, 1028.
- (28) Kagan, C. R.; Murray, C. B.; Bawendi, M. G. *Phys. Rev. B* **1996**, *54*, 8633.
- (29) Varshni, Y. P. *Physica* **1967**, *34*, 149.
- (30) Fan, H. Y. *Phys. Rev.* **1951**, *82*, 900.
- (31) Morello, G.; De Giorgi, M.; Kudera, S.; Manna, L.; Cingolani, R.; Anni, M. *J. Phys. Chem. C* **2007**, *111*, 5846.
- (32) Al Salman, A.; Tortschanoff, A.; Mohamed, M. B.; Tonti, D.; van Mourik, F.; Chergui, M. *Appl. Phys. Lett.* **2007**, *90*, 093104.
- (33) Valerini, D.; Creti, A.; Lomascolo, M.; Manna, L.; Cingolani, R.; Anni, M. *Phys. Rev. B* **2005**, *71*, 235409.
- (34) Laheld, U. E. H.; Pedersen, F. B.; Hemmer, P. C. *Phys. Rev. B* **1993**, *48*, 4659.
- (35) Cho, Y. H.; Gainer, G. H.; Fischer, A. J.; Song, J. J.; Keller, S.; Mishra, U. K.; DenBaars, S. P. *Appl. Phys. Lett.* **1998**, *73*, 1370.
- (36) Hong, Y. G.; Nishikawa, A.; Tu, C. W. *Appl. Phys. Lett.* **2003**, *83*, 5446.
- (37) Tönnies, D.; Bacher, G.; Forchel, A.; Waag, A.; Litz, Th.; Hommel, D.; Becker, Ch.; Landwehr, G.; Heukens, M.; Scholl, M. *J. Cryst. Growth* **1994**, *138*, 362.
- (38) Bailey, R. E.; Nie, S. J. *Am. Chem. Soc.* **2003**, *125*, 7100.
- (39) Smith, A. M.; Mohs, A. M.; Nie, S. *Nat. Nanotechnol.* **2009**, *4*, 56.
- (40) Ithurria, S.; Guyot-Sionnest, P.; Mahler, B.; Dubertret, B. *Phys. Rev. Lett.* **2007**, *99*, 265501.
- (41) Hellwege, K. H. *Landolt-Börnstein Numerical Data and Functional Relationship in Science and Technology*; Springer-Verlag: Berlin, 1982.
- (42) Lee, J.; Koteles, E. S.; Vassell, M. O. *Phys. Rev. B* **1986**, *33*, 5512.
- (43) Vinogradov, V. S.; Karczewski, G.; Kucherenko, I. V.; Mel'nik, N. N.; Fernandez, P. *Phys. Solid State* **2008**, *50*, 164.
- (44) Rudin, S.; Reinecke, T. L.; Segall, B. *Phys. Rev. B* **1990**, *42*, 11218.
- (45) Toyozawa, Y.; Hermanson, J. *Phys. Rev. B* **1968**, *21*, 1637.
- (46) Alivisatos, A. P.; Harris, T. S.; Carroll, P. J.; Steigerwald, M. I.; Brus, I. E. *J. Chem. Phys.* **1989**, *90*, 3463.
- (47) Nirmal, M.; Dabbousi, B.; Bawendi, M.; Macklin, J.; Trautman, J.; Harris, T.; Brus, L. *Nature (London)* **1996**, *383*, 802.
- (48) Rosen, S.; Schwartz, O.; Oron, D. *Phys. Rev. Lett.* **2010**, *104*, 157404.
- (49) Wang, S.; Querner, C.; Emmons, T.; Drndic, M.; Crouch, C. H. *J. Phys. Chem. B* **2006**, *110*, 23221.
- (50) Kim, Y.; Song, N. W.; Yu, H.; Moon, D. W.; Lim, S. J.; Kim, W.; Yoon, H.-J.; Shin, S. K. *Phys. Chem. Chem. Phys.* **2009**, *11*, 3497.
- (51) Gómez, D. E.; van Embden, J.; Jasieniak, J.; Smith, T. A.; Mulvaney, P. *Small* **2006**, *2*, 204.
- (52) Chon, B.; Lim, S. J.; Kim, W.; Seo, J.; Kang, H.; Joo, T.; Hwang, J.; Shin, S. K. *Phys. Chem. Chem. Phys.* **2010**, *12*, 9312.
- (53) Shimizu, K. T.; Neuhauser, R. G.; Leatherdale, C. A.; Empedocles, S. A.; Woo, W. K.; Bawendi, M. G. *Phys. Rev. B* **2001**, *63*, 205311.
- (54) Efros, A. L.; Rosen, M. *Phys. Rev. Lett.* **1997**, *78*, 1110.
- (55) Verberk, R.; van Oijen, A. M.; Orrit, M. *Phys. Rev. B* **2002**, *66*, 233202.
- (56) Tang, J.; Marcus, R. A. *Phys. Rev. Lett.* **2005**, *95*, 107401.
- (57) Margolin, G.; Protasenko, V.; Kuno, M.; Barkai, E. *Adv. Chem. Phys.* **2006**, *133*, 327.